Spatial Sectorized Neural Network for 2-D DOA Estimation in the Full Azimuth

Feiyang Qian[†], Hang Zheng[†,‡], Chengwei Zhou[†,‡], and Zhiguo Shi[†,♯]
[†]State Key Laboratory of Industrial Control Technology, Zhejiang University, Hangzhou 310027, China
[‡]Key Laboratory of Collaborative Sensing and Autonomous Unmanned Systems of Zhejiang Province, Hangzhou 310015, China
[♯]Jinhua Institute of Zhejiang University, Jinhua 321037, China
E-mail: qianfy@zju.edu.cn, hangzheng@zju.edu.cn, zhouchw@zju.edu.cn, shizg@zju.edu.cn

***Abstract*—Most existing deep learning-based direction-of-arrival (DOA) estimation methods are realized within a limited range of DOAs per training time, posing great challenges to effective DOA estimation in a full 3-D space of 360°. To address the problem, a spatial sectorized neural network is proposed for 2-D DOA estimation in the full azimuth. In particular, the full angular region is divided into a series of sectors to compress the ranges of both azimuth and elevation angles. Based on that, we formulate the full-azimuth DOA estimation problem into two tasks, namely, sector identification and angles mapping. To this end, the proposed network consists of a classifier and an estimator, thereby addressing the issue of angle discontinuity near the 0° and 360°. The estimated DOAs can be reconstructed from the outputs of the proposed network based on the angles mapping relationship, leading to an effective 2-D DOA estimation in the full azimuth. Our simulation results indicate that the proposed network outperforms the conventional model-based method and neural-network-based method in estimation accuracy.**

***Index Terms*—DOA estimation, full azimuth, neural network, spatial sectorization.**

I. Introduction

Direction-of-arrival (DOA) estimation plays a fundamental role in various applications, including radar, wireless communication, Internet of Things (IoT), and astronomy [1], [2], [3], [4], [5], [6]. Conventional model-based DOA estimation, such as MUSIC [7], ESPRIT [8], sparsity-based [9], [10], [11], and tensor-based methods [12], [13], [14], are typically based on statistical optimizations. However, as the signal propagation environments becoming more complicated, these model-based methods suffer from degraded estimation accuracy and lower computational efficiency. To address the problem, deep learning-based DOA estimation methods have been developed to handle diverse scenarios, including multipath propagation [15], [16], non-Gaussian interference [17], coherent sources [18], array imperfections [19], few snapshots [20], limited system resources [21], [22], [23] and others [24], [25], [26], [27], [28]. However, most of these methods are completed within preset limited ranges of azimuth and elevation angles to pursue a satisfactory performance. While, sources in the 3-D space may emit signals from any potential angle of 360° relative to the antenna array, in such case, the performance of the aforementioned deep learning techniques degrades when the range of DOAs expands.

Concerning the above-mentioned issue, a series of approaches have been proposed for 2-D DOA estimation in the full azimuth. In [29], full-azimuth DOA estimation is accomplished using two distinct beam scanning procedures. Based on the extended manifold separation technique, the 3-D spatial-temporal spectrum is computed and an estimator called FFT-MUSIC is proposed to realize 2-D DOA estimation in the full azimuth [30]. In [31], a sparse array design is investigated, which allows to estimate the DOAs of more sources than the number of antennas in full azimuth field-of-view. Nevertheless, these model-based methods are time-consuming and sensitive to noise. In this regard, a CNN-based classifier is employed in [32] to estimate wider ranges of azimuth angles, but the complexity of the network is unacceptable when additional elevation angle information is required. Although sparse Bayesian learning can be adopted to aid the full-azimuth DOA estimation task [33], it is only suitable for the high signal-to-noise ratio (SNR) environments. Thus, it remains an outstanding but challenging problem in designing an effective neural network for 2-D DOA estimation in the full azimuth.

In this paper, a spatial sectorized neural network is proposed for full-azimuth DOA estimation. Specifically, the full angular region is divided into a group of sectors to compress the wide range of DOAs. Then, the azimuth and elevation angles are mapped into a limited angular range by encoding sectors. A classification and a regression neural networks are designed to estimate the sector indices and the DOAs after mapping, respectively. As such, the impact of wide angle range is eliminated by the connected classification and regression networks, which behaves less sensitive to the DOA range discontinuity compared to the conventional networks. Estimations of azimuth and elevation angles are reconstructed by the outputs of the proposed spatial sectorized neural network, enabling the effective 2-D DOA estimation in the full azimuth. Simulation results corroborate the superiority of the proposed network over the model-based method and the existing network.

This work was partially supported by Zhejiang Jianbing Plan (2022C01028), Fundamental Research Funds for the Central Universities (226-2023-00111, 226-2024-00004), National Natural Science Foundation of China (U21A20456, 62271444), and the Zhejiang University Education Foundation Qizhen Scholar Foundation.

II. Signal Model

We consider a uniform rectangular array (URA) $\mathbb{P}$ with $M \times N$ antennas, where M and N respectively denote the number of antennas along the x-axis and the y-axis. The inter-element spacing of $\mathbb{P}$ is half of the signal wavelength. Assume that K uncorrelated farfield narrowband source signals impinge on $\mathbb{P}$ from directions $\{(\theta_k, \phi_k), k = 1, 2, \ldots, K\}$, where $\theta_k \in [0°, 360°]$ and $\phi_k \in [0°, 90°]$ denote the azimuth and elevation angles of the k-th source, respectively. Here, the DOAs of sources are assumed to lie within the full azimuth, instead of a relatively narrow region as the conventional assumptions.

The array received signals can be modeled as a matrix

$$\boldsymbol{X} = \boldsymbol{A}\boldsymbol{S} + \boldsymbol{N} \in \mathbb{C}^{MN \times T}, \tag{1}$$

where $\boldsymbol{S} = [\boldsymbol{s}_1, \boldsymbol{s}_2, \cdots, \boldsymbol{s}_K]^{\mathrm{T}} \in \mathbb{C}^{K \times T}$ is the signal matrix of K sources with $\boldsymbol{s}_k = [s_k(1), s_k(2), \cdots, s_k(T)] \in \mathbb{C}^T$ being the signal waveform of the k-th source, T is the number of snapshots, $\boldsymbol{A} = [\boldsymbol{a}_1, \boldsymbol{a}_2, \cdots, \boldsymbol{a}_K] \in \mathbb{C}^{MN \times K}$ is the steering matrix with

$$\boldsymbol{a}_k = \left[1, e^{-\jmath\pi(M-1)\mu_k}, \cdots, e^{-\jmath\pi(M-1)\mu_k - \jmath\pi(N-1)\nu_k}\right]^{\mathrm{T}} \in \mathbb{C}^{MN} \tag{2}$$

being the steering vector of the k-th source, and $\boldsymbol{N}$ is the additive Gaussian white noise. Here, $\mu_k = \sin\phi_k \cos\theta_k$, $\nu_k = \sin\phi_k \sin\theta_k$, $\jmath$ denotes the imaginary unit, and $[\cdot]^{\mathrm{T}}$ denotes the transpose operator.

To extract the spatial correlation information from signals while reducing the input dimensionality, the covariance matrix

$$\boldsymbol{R} = \mathrm{E}\left\{\frac{1}{T}\boldsymbol{X}\boldsymbol{X}^{\mathrm{H}}\right\} = \boldsymbol{A}^{\mathrm{H}}\boldsymbol{R}_s\boldsymbol{A} + \sigma_n^2\boldsymbol{I} \in \mathbb{C}^{MN \times MN}, \tag{3}$$

is derived as the input of the neural network, where $\boldsymbol{R}_s = \mathrm{E}\{\frac{1}{T}\boldsymbol{S}\boldsymbol{S}^{\mathrm{H}}\} \in \mathbb{C}^{K \times K}$ is the covariance matrix of source signals, σ_n^2 is the power of noise, $[\cdot]^{\mathrm{H}}$, $\mathrm{E}\{\cdot\}$ and $\boldsymbol{I}$ respectively denote the conjugate transpose operator, the statistical expectation and the identity matrix. In practice, $\boldsymbol{R}$ is approximated by

$$\hat{\boldsymbol{R}} = \frac{1}{T}\boldsymbol{X}\boldsymbol{X}^{\mathrm{H}}. \tag{4}$$

It is noteworthy that existing deep learning framework, such as PyTorch, can only handle real-valued data. In this regard, we stack the real and imaginary parts of $\hat{\boldsymbol{R}}$ along a new dimention to build a 3-D tensor input, which can be fed into the neural network to retrieve azimuth and elevation angles for 2-D DOA estimation in the full azimuth.

III. Proposed Network for DOA Estimation

In this section, we propose a spatial sectorized neural network to realize full-azimuth DOA estimation. Specifically, the pair of azimuth and elevation angles is mapped to a triplet, which consists of the sector information and the angles after mapping. This constrains the azimuth and elevation angles to a relatively narrow range. Accordingly, a pair of interconnected neural networks is designed to classify sector indices and estimate DOAs after mapping. The original azimuth and elevation angles are reconstructed by the triplet, thereby facilitating 2-D DOA estimation in the full azimuth.

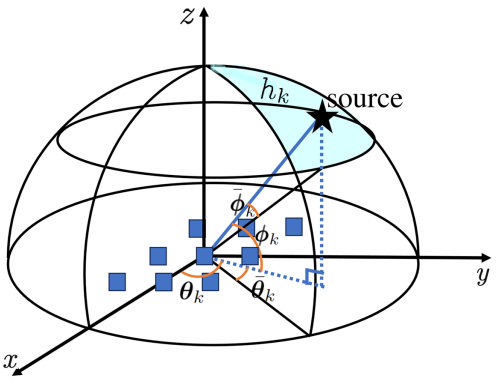

Fig. 1: Spatial sectorization for azimuth and elevation mapping.

A. Spatial Sectorization and Angles Mapping

In DOA estimation tasks, classification and regression networks are widely applied. However, when the range of DOAs expands, numerous classes are required in the classification network, which results in excessive computational complexity. As for the regression network, the accuracy declines when facing sources near the $0°$ and $360°$ due to the range discontinuity. To maintain a high accuracy of full-azimuth DOA estimation, it is necessary to compress the wide ranges of DOA into narrow ones. Thus, spatial sectorization and angles mapping are proposed.

Specifically, the range of the azimuth angle is sectorized into P subregions with an equal size, and the range of the elevation angle is also equally sectorized into Q subregions. As such, the entire angular space is partitioned into $P \times Q$ equally sized sectors. The DOA of the k-th source belongs to a specific sector, denoted by an index h_k, which can be calculated as

$$h_k = \left\lfloor \frac{\theta_k}{A_\theta} \right\rfloor + P \left\lfloor \frac{\phi_k}{A_\phi} \right\rfloor \in [0, PQ - 1]. \tag{5}$$

Here,

$$A_\theta = \frac{360°}{P}, \; A_\phi = \frac{90°}{Q} \tag{6}$$

respectively denote the range of azimuth and elevation angles of each sector, and $\lfloor \cdot \rfloor$ denotes the floor function.

Let $\boldsymbol{\theta} = [\theta_1, \theta_2 \cdots, \theta_K]$, $\boldsymbol{\phi} = [\phi_1, \phi_2 \cdots, \phi_K]$, as shown in Fig. 1, the relationship between $\{\boldsymbol{\theta}, \boldsymbol{\phi}\}$ and the DOAs after sectorization, i.e., $\{\bar{\boldsymbol{\theta}}, \bar{\boldsymbol{\phi}}\}$, can be expressed as

$$\bar{\boldsymbol{\theta}} = \boldsymbol{\theta} - A_\theta \left\lfloor \frac{\boldsymbol{\theta}}{A_\theta} \right\rfloor = \boldsymbol{\theta} - A_\theta(\boldsymbol{h} \bmod P) \in [0, A_\theta), \tag{7}$$

$$\bar{\boldsymbol{\phi}} = \boldsymbol{\phi} - A_\phi \left\lfloor \frac{\boldsymbol{\phi}}{A_\phi} \right\rfloor = \boldsymbol{\phi} - A_\phi \left\lfloor \frac{\boldsymbol{h}}{P} \right\rfloor \in [0, A_\phi), \tag{8}$$

where $\bar{\boldsymbol{\theta}} = [\bar{\theta}_1, \bar{\theta}_2, \cdots, \bar{\theta}_K]$, $\bar{\boldsymbol{\phi}} = [\bar{\phi}_1, \bar{\phi}_2, \cdots, \bar{\phi}_K]$, $\bar{\theta}_k$ and $\bar{\phi}_k$ respectively denote the sectorized azimuth and elevation angles of the k-th source, $\mathrm{mod}(\cdot)$ denotes the modulo operator,

$\boldsymbol{h} = [h_1, h_2, \cdots, h_K]$ denotes the sector indices. As such, the DOAs $\{\boldsymbol{\theta}, \boldsymbol{\phi}\}$ can now be equivalently characterized by the triplet $\{\boldsymbol{h}, \bar{\boldsymbol{\theta}}, \bar{\boldsymbol{\phi}}\}$ after angles mapping process.

Notably, by introducing the sector indices $\boldsymbol{h}$, the maximum values of $\{\bar{\boldsymbol{\theta}}, \bar{\boldsymbol{\phi}}\}$ are restricted to $\max\{A_\theta, A_\phi\}$, whose angular range is much smaller than $\{\boldsymbol{\theta}, \boldsymbol{\phi}\}$. Based on this property, a spatial sectorized neural network is designed for full-azimuth DOA estimation.

B. Spatial Sectorized Neural Network Framework

In order to accommodate the designed sectorization process, the proposed network consists of a classification neural network called *Classifier* and a regression neural network called *Estimator*. In particular, *Classifier* and *Estimator* are employed to estimate the sector information $\boldsymbol{h}$ and the sectorized DOA $\{\bar{\boldsymbol{\theta}}, \bar{\boldsymbol{\phi}}\}$, respectively. Based on the principle of spatial sectorization, the required number of classes for *Classifier* is relatively small after sectorization. Meanwhile, in *Estimator*, the range of $\{\bar{\boldsymbol{\theta}}, \bar{\boldsymbol{\phi}}\}$ is compressed and the range discontinuity of DOA near 0° and 360° can be evaded. Thus, the impact of DOA range expansion is eliminated, which contributes to a stable performance in the full-azimuth scenario. Besides, the powerful fitting and generalization capabilities of the proposed network ensure a low computational complexity with robustness to noise, compared to the model-based method.

The architecture of the proposed spatial sectorized neural network is shown in Fig. 2. Both *Classifier* and *Estimator* utilize the covariance matrix of signals as input. For *Classifier*, convolutional layers and a multilayer perceptron (MLP) are deployed. The output of *Classifier* is K probability distributions of PQ sectors. Therefore, K Softmax functions are followed by the output layer. Sector indices $\boldsymbol{h}$ can be obtained by extracting the indices corresponding to the maximum value among each PQ neurons in the output layer. For *Estimator*, convolutional layers are stacked. The expected output of *Estimator* is a vector $\bar{\boldsymbol{\vartheta}} = [\bar{\theta}_1, \bar{\theta}_2, \cdots, \bar{\theta}_K, \bar{\phi}_1, \bar{\phi}_2, \cdots, \bar{\phi}_K]$, i.e., $\{\bar{\boldsymbol{\theta}}, \bar{\boldsymbol{\phi}}\}$. Note that pooling layers are not necessary for the proposed network since the depth of the network framework is shallow to prevent excessive model complexity.

C. Network Training and 2-D DOA Reconstruction

In the training stage, *Classifier* and *Estimator* are trained independently. The loss function of *Classifier* is the binary cross-entropy function, i.e.,

$$\mathrm{E_c}(\boldsymbol{p}, \hat{\boldsymbol{p}}) = -\frac{1}{C}\sum_{j=1}^{C}\Big[p_j \log \hat{p}_j + (1-p_j)\log(1-\hat{p}_j)\Big], \quad (9)$$

where $C = KPQ$ denotes the number of output layer neurons, $\boldsymbol{p} = [p_1, p_2, \cdots, p_C] \in \{0, 1\}$ and $\hat{\boldsymbol{p}} = [\hat{p}_1, \hat{p}_2, \cdots, \hat{p}_C] \in [0, 1]$ respectively denote the true and estimated probability of sectors. Assuming that the maximum value in the probability distribution corresponds to the matched sector of the input signal, the sector indices can be estimated by

$$h_k = \underset{(k-1)PQ < i \leqslant kPQ}{\arg\max} \; p_i. \quad (10)$$

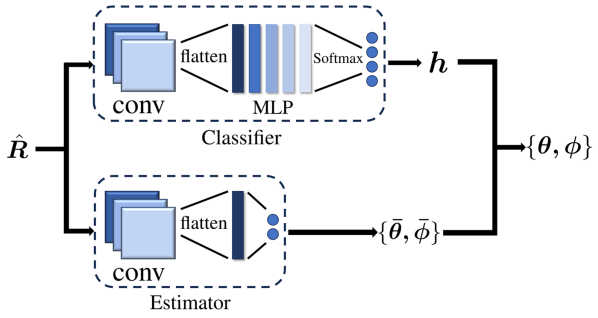

Fig. 2: The proposed spatial sectorized neural network.

To train *Estimator*, we utilize Huber function as the loss function, i.e.,

$$\mathrm{E_r}(\bar{\boldsymbol{\vartheta}}, \hat{\bar{\boldsymbol{\vartheta}}}) = \begin{cases} \frac{1}{4K}\|\bar{\boldsymbol{\vartheta}} - \hat{\bar{\boldsymbol{\vartheta}}}\|_2, & \text{if} \|\bar{\boldsymbol{\vartheta}} - \hat{\bar{\boldsymbol{\vartheta}}}\|_1 \leqslant K\eta, \\ \frac{1}{2K}\left(\|\bar{\boldsymbol{\vartheta}} - \hat{\bar{\boldsymbol{\vartheta}}}\|_1 - \frac{1}{2}\eta\right), & \text{otherwise}, \end{cases} \quad (11)$$

where $\hat{\bar{\boldsymbol{\vartheta}}} = [\hat{\bar{\theta}}_1, \hat{\bar{\theta}}_2, \cdots, \hat{\bar{\theta}}_K, \hat{\bar{\phi}}_1, \hat{\bar{\phi}}_2, \cdots, \hat{\bar{\phi}}_K]$ contains the estimated DOAs of signals. $\|\cdot\|_1$ and $\|\cdot\|_2$ respectively denote the Taxicab norm and Euclidean norm, and η is a threshold to control the value of Huber loss between the mean squared error (MSE) and the mean absolute error (MAE), making the Huber function more robust than MSE or MAE losses. The parameter matrices of *Classifier* and *Estimator* can be updated with gradient descent method, which is controlled by the learning rate $\alpha > 0$.

Once $\boldsymbol{h}$ and $\{\bar{\boldsymbol{\theta}}, \bar{\boldsymbol{\phi}}\}$ are estimated by the proposed network, the estimated azimuth and elevation angles $\{\hat{\boldsymbol{\theta}}, \hat{\boldsymbol{\phi}}\}$ can be reconstructed according to the angles mapping relationship (7) and (8), i.e.,

$$\hat{\boldsymbol{\theta}} = \hat{\bar{\boldsymbol{\theta}}} + (\hat{\boldsymbol{h}} \bmod P) \times A_\theta, \quad (12)$$

$$\hat{\boldsymbol{\phi}} = \hat{\bar{\boldsymbol{\phi}}} + \left\lfloor \frac{\hat{\boldsymbol{h}}}{P} \right\rfloor \times A_\phi, \quad (13)$$

where $\hat{\boldsymbol{h}}$ and $\{\hat{\bar{\boldsymbol{\theta}}}, \hat{\bar{\boldsymbol{\phi}}}\}$ respectively denote the estimated sectors and angles from the output layers of the proposed network. In summary, through the angles mapping, the designed spatial sectorized neural network, and the corresponding 2-D DOA reconstruction, the full-azimuth DOA estimation is consequently accomplished.

IV. Simulation

In the simulations, we consider a URA with $M = N = 7$ and the number of signals $K = 1$. The number of snapshots is fixed at $T = 250$, and the size of input tensor is $49 \times 49 \times 2$. The choice of P, Q is a trade-off between *Classifier*'s accuracy and *Estimator*'s precision. Excessive sector identification error leads to a degradation in DOA estimation, which overshadows the performance gain of *Estimator* within smaller sector ranges. Considering this, we select $P = 8$ and $Q = 2$.

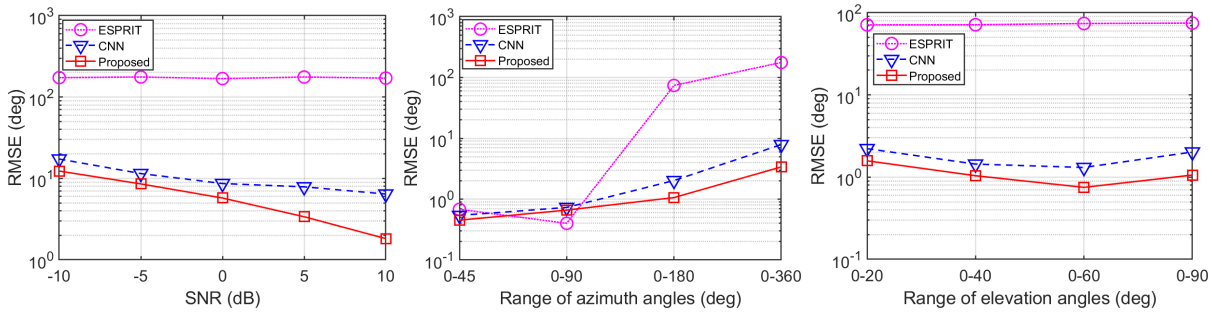

(a) (b) (c)

Fig. 3: DOA estimation performance comparison. (a) RMSE versus SNR with $\theta \in [0°, 360°]$. (b) RMSE versus the range of θ with SNR = 5dB and $\phi \in [0°, 90°]$. (c) RMSE versus the range of ϕ with SNR = 5dB and $\theta \in [0°, 180°]$.

In particular, two convolutional layers and five fully connected layers are used in the deployed *Classifier*, and $\mathrm{ReLU}(\cdot)$ is chosen as the activation function. For *Estimator*, three convolutional layers are set. $\mathrm{Tanh}(\cdot)$ is selected for the first activation function, and $\mathrm{ReLU}(\cdot)$ is used for the remaining activation functions. Detailed information of network layers is shown in TABLE I and TABLE II.

TABLE I: Description of layers in *Classifier*

Layer	Description
Conv1	channels: 16, kernel size: (3×3), padding: (1,1)
Conv2	channels: 32, kernel size: (3×3), padding: (0,0)
Flatten	reshape 3-D tensor into a vector
Fc1&Fc3&Fc5	512 neurons
Fc2&Fc4	128 neurons
Output	16 neurons with a Softmax

TABLE II: Description of layers in *Estimator*

Layer	Description
Conv1	channels: 16, kernel size: (5×5), padding: (1,1)
Conv2	channels: 32, kernel size: (5×5), padding: (0,0)
Conv3	channels: 32, kernel size: (3×3), padding: (0,0)
Flatten	reshape 3-D tensor into a vector
Output	2 neurons

We generate $40,500$ samples as the dataset to train both *Classifier* and *Estimator*. For each sample, azimuth and elevation angles $\{\boldsymbol{\theta}, \boldsymbol{\phi}\}$ are respectively chosen within the ranges of $[0°, 360°]$ and $[0°, 90°]$ randomly, so that $A_\theta = A_\phi = 45°$. The SNR of signals is randomly selceted from the set $\{-10, -5, 0, 5, 10\}$ dB. The threshold η for Huber loss in (11) is set to 1. Adam[34] is chosen for the optimizer of both *Classifier* and *Estimator*. The number of training epochs and batch size are respectively set to 40 and 32. Learning rate is set to 5×10^{-4} during the first 30 epochs and will reduce to 5×10^{-5} for the last 10 epochs. The deployed network is run on a computer equipped with an NVIDIA GeForce RTX 3060 Laptop GPU. Meanwhile, a CNN is deployed to directly estimate the full-azimuth DOA, serving as the benchmark. The architecture and hyperparameters of CNN are identical to those of *Estimator*.

In Fig. 3, we compare the estimation accuracy of the proposed network to those of the conventional CNN and ESPRIT. The root-mean-square error (RMSE) is chosen as the performance metric for comparison. To produce the curves, $10,000$ Monte Carlo trials are performed for each scenario. As depicted in Fig. 3(a), the proposed network has an improved estimation accuracy compared to the CNN in all tested scenarios. The RMSE of the CNN is about $6.5°$ even in a relatively high SNR scenario (SNR = 10 dB), which indicates that the conventional network faces challenges in handling full-azimuth scenario. By contrast, the proposed network exhibits a 71.7% improvement in estimation accuracy compared to the CNN when SNR = 10 dB. The total RMSE of the proposed network is acceptable as *Classifier* can maintain a high accuracy in sectors classification. As shown in Fig. 3(b) and Fig. 3(c), the RMSE of both the CNN and ESPRIT increases when the ranges of azimuth and elevation angles become larger, whereas the RMSE of the proposed network maintains a relatively stable trend.

TABLE III: *Classifier* and *Estimator* performance versus SNR

SNR (dB)	-10	-5	0	5	10
Classifier: Accuracy (%)	96.9	98.4	99.0	99.3	99.6
Estimator: RMSE (deg)	1.39	0.88	0.67	0.53	0.41

In TABLE III, we list the classification accuracy of *Classifier* and the RMSE of *Estimator* versus SNR when $\theta \in [0°, 360°]$ and $\phi \in [0°, 90°]$. It is clear that both *Classifier* and *Estimator* maintain a robust performance, being less sensitive to the range of DOAs compared to the conventional methods. Therefore, the effectiveness of the proposed method in handling full-azimuth DOA estimation is verified.

V. Conclusion

In this paper, we proposed a spatial sectorized neural network for full-azimuth DOA estimation. By dividing the full angular space into sectors, the range of DOAs is compressed to avoid the angle discontinuity. The proposed network consists of *Classifier* for sector identification and *Estimator* for angles mapping. Simulation results corroborate the enhanced DOA estimation accuracy of the proposed method compared to the conventional model-based method and the CNN.

REFERENCES

[1] H. L. Van Trees, *Detection, Estimation, and Modulation Theory, Part IV: Optimum Array Processing*. New York, NY, USA: Wiley, 2002.

[2] W. Liu, M. Haardt, M. S. Greco, C. F. Mecklenbräuker, and P. Willett, "Twenty-five years of sensor array and multichannel signal processing: A review of progress to date and potential research directions," *IEEE Signal Process. Mag.*, vol. 40, no. 4, pp. 80–91, June 2023.

[3] C. Zhou, Y. Gu, X. Fan, Z. Shi, G. Mao, and Y. D. Zhang, "Direction-of-arrival estimation for coprime array via virtual array interpolation," *IEEE Trans. Signal Process.*, vol. 66, no. 22, pp. 5956–5971, 2018.

[4] S. He, K. Shi, C. Liu, B. Guo, J. Chen, and Z. Shi, "Collaborative sensing in internet of things: A comprehensive survey," *IEEE Commun. Surv. Tutorials*, vol. 24, no. 3, pp. 1435–1474, 2022.

[5] C. Yang, L. Feng, H. Zhang, S. He, and Z. Shi, "A novel data fusion algorithm to combat false data injection attacks in networked radar systems," *IEEE Trans. Signal Inf. Process. Networks*, vol. 4, no. 1, pp. 125–136, 2018.

[6] Z. Shi, X. Chang, C. Yang, Z. Wu, and J. Wu, "An acoustic-based surveillance system for amateur drones detection and localization," *IEEE Trans. Veh. Technol.*, vol. 69, no. 3, pp. 2731–2739, 2020.

[7] R. Schmidt, "Multiple emitter location and signal parameter estimation," *IEEE Trans. Antennas Propag.*, vol. 34, no. 3, pp. 276–280, 1986.

[8] R. Roy and T. Kailath, "ESPRIT-estimation of signal parameters via rotational invariance techniques," *IEEE Trans. Acoust., Speech, Signal Process.*, vol. 37, no. 7, pp. 984–995, 1989.

[9] Y. D. Zhang, M. G. Amin, and B. Himed, "Sparsity-based DOA estimation using co-prime arrays," in *Proc. IEEE Int. Conf. Acoust., Speech, Signal Process. (ICASSP)*, Vancouver, BC, Canada, May 2013.

[10] C. Zhou, Y. Gu, Z. Shi, and M. Haardt, "Structured Nyquist correlation reconstruction for DOA estimation with sparse arrays," *IEEE Trans. Signal Process.*, vol. 71, pp. 1849–1862, 2023.

[11] X. Wu and W.-P. Zhu, "On efficient gridless methods for 2-D DOA estimation with uniform and sparse L-shaped arrays," *Signal Process.*, vol. 191, p. 108351, 2022.

[12] H. Zheng, C. Zhou, Z. Shi, Y. Gu, and Y. D. Zhang, "Coarray tensor direction-of-arrival estimation," *IEEE Trans. Signal Process.*, vol. 71, pp. 1128–1142, 2023.

[13] F. Xu, M. W. Morency, and S. A. Vorobyov, "DOA estimation for transmit beamspace MIMO radar via tensor decomposition with vandermonde factor matrix," *IEEE Trans. Signal Process.*, vol. 70, pp. 2901–2917, 2022.

[14] H. Zheng, C. Zhou, Z. Shi, and Y. Gu, "Structured tensor reconstruction for coherent DOA estimation," *IEEE Signal Process. Lett.*, vol. 29, pp. 1634–1638, 2022.

[15] J. Yu and Y. Wang, "Deep learning-based multipath DoAs estimation method for mmWave massive MIMO systems in low SNR," *IEEE Trans. Veh. Technol.*, vol. 72, no. 6, pp. 7480–7490, 2023.

[16] H. Xiang, B. Chen, T. Yang, and D. Liu, "Improved de-multipath neural network models with self-paced feature-to-feature learning for DOA estimation in multipath environment," *IEEE Trans. Veh. Technol.*, vol. 69, no. 5, pp. 5068–5078, 2020.

[17] S. Feintuch, J. Tabrikian, I. Bilik, and H. Permuter, "Neural-network-based DOA estimation in the presence of non-Gaussian interference," *IEEE Trans. Aerosp. Electron. Syst.*, vol. 60, no. 1, pp. 119–132, 2024.

[18] H. Xiang, B. Chen, M. Yang, and S. Xu, "Angle separation learning for coherent DOA estimation with deep sparse prior," *IEEE Commun. Lett.*, vol. 25, no. 2, pp. 465–469, 2021.

[19] Z.-M. Liu, C. Zhang, and P. S. Yu, "Direction-of-arrival estimation based on deep neural networks with robustness to array imperfections," *IEEE Trans. Antennas Propag.*, vol. 66, no. 12, pp. 7315–7327, 2018.

[20] Y. Ma, Y. Zeng, and S. Sun, "A deep learning based super resolution DoA estimator with single snapshot MIMO radar data," *IEEE Trans. Veh. Technol.*, vol. 71, no. 4, pp. 4142–4155, 2022.

[21] H. Zheng, C. Zhou, S. A. Vorobyov, and Z. Shi, "Tensorized neural layer decomposition for 2-D DOA estimation," in *Proc. IEEE Int. Conf. Acoust., Speech, Signal Process. (ICASSP)*, Rhodes Island, Greece, June 2023.

[22] C. Shi, Z. Tang, L. Ding, and J. Yan, "Multidomain resource allocation for asynchronous target tracking in heterogeneous multiple radar networks with non-ideal detection," *IEEE Trans. Aerosp. Electron. Syst.*, vol. 60, no. 2, pp. 2016–2033, 2024.

[23] H. Zheng, C. Zhou, S. A. Vorobyov, Q. Wang, and Z. Shi, "Decomposed CNN for sub-Nyquist tensor-based 2-D DOA estimation," *IEEE Signal Process. Lett.*, vol. 30, pp. 708–712, 2023.

[24] X. Wu, X. Yang, X. Jia, and F. Tian, "A gridless DOA estimation method based on convolutional neural network with Toeplitz prior," *IEEE Signal Process. Lett.*, vol. 29, pp. 1247–1251, 2022.

[25] H. Zheng, Z. Shi, C. Zhou, M. Haardt, and J. Chen, "Coupled coarray tensor CPD for DOA estimation with coprime L-shaped array," *IEEE Signal Process. Lett.*, vol. 28, pp. 1545–1549, 2021.

[26] R. Varzandeh, S. Doclo, and V. Hohmann, "Speech-aware binaural DOA estimation utilizing periodicity and spatial features in convolutional neural networks," *IEEE/ACM Trans. Audio Speech Lang. Process.*, vol. 32, pp. 1198–1213, 2024.

[27] R. Zheng, H. Liu, S. Sun, and J. Li, "Deep learning based computationally efficient unrolling IAA for direction-of-arrival estimation," in *Proc. European Signal Process. Conf. (EUSIPCO)*, Helsinki, Finland, Sept. 2023, pp. 730–734.

[28] H. Zheng, Z. Shi, C. Zhou, and A. L. F. de Almeida, "Coarray tensor completion for DOA estimation," *IEEE Trans. Aerosp. Electron. Syst.*, vol. 59, no. 5, pp. 5472–5486, Oct. 2023.

[29] S. Abielmona, H. V. Nguyen, and C. Caloz, "Analog direction of arrival estimation using an electronically-scanned CRLH leaky-wave antenna," *IEEE Trans. Antennas Propag.*, vol. 59, no. 4, pp. 1408–1412, 2011.

[30] L. Chen, W. Qi, P. Liu, E. Yuan, Y. Zhao, and G. Ding, "Low-complexity joint 2-D DOA and TOA estimation for multipath OFDM signals," *IEEE Signal Process. Lett.*, vol. 26, no. 11, pp. 1583–1587, 2019.

[31] M. Rubsamen and A. B. Gershman, "Sparse array design for azimuthal direction-of-arrival estimation," *IEEE Trans. Signal Process.*, vol. 59, no. 12, pp. 5957–5969, 2011.

[32] S. Chakrabarty and E. A. Habets, "Multi-scale aggregation of phase information for complexity reduction of CNN based DOA estimation," in *Proc. European Signal Process. Conf. (EUSIPCO)*, A Coruña, Spain, Sept. 2019.

[33] G. Ping, E. Fernandez Grande, P. Gerstoft, and Z. Chu, "Three-dimensional source localization using sparse Bayesian learning on a spherical microphone array," *J. Acoust. Soc. Am.*, vol. 147, no. 6, pp. 3895–3904, 2020.

[34] D. P. Kingma and J. Ba, "Adam: A method for stochastic optimization," in *Proc. Int. Conf. Learn. Represent. (ICLR)*, San Diego, CA, May 2015.